F 2   Imaging with X-rays, Neutrons and Synchrotron Radiation

E. H. Lehmann

Neutron Imaging & Activation Group

Spallation Neutron Source Division

Paul Scherrer Institut, Switzerland

Contents

1   Introduction

More than one century ago, Konrad Röntgen discovered X-rays and their performance – by means of imaging methods. His first pictures of human bones inside the body initiated a revolution in medical inspections. It is still common in all hospitals on very routine basis to perform transmission images of parts of the patient's body to find abnormalities and defects.

The use of X-rays for material research on the microscopic and atomic scale was initiated by Laue, Bragg and Debye more than ten years later. Even than, X-ray films were used initially for the investigation of the diffraction rings and spots around the crystalline samples.

The discovery of neutrons (Chadwick) came about 40 years after Röntgen's experiments and found most interests in atomic physics, reactor physics, nuclear weapon programs and radiochemistry. The hype for nuclear weapons at the end of the Second World War and the installation of reactors provided also the access to beams of free neutrons. However, first neutron images were done in Berlin by Kalman and Kuhn at an accelerator driven neutron source.

Because the radiography with X-rays and neutrons were done until about 1970 exclusively with film methods, the applications were limited in respect to the frame rate, the image quality and the introduction of more advanced methods.
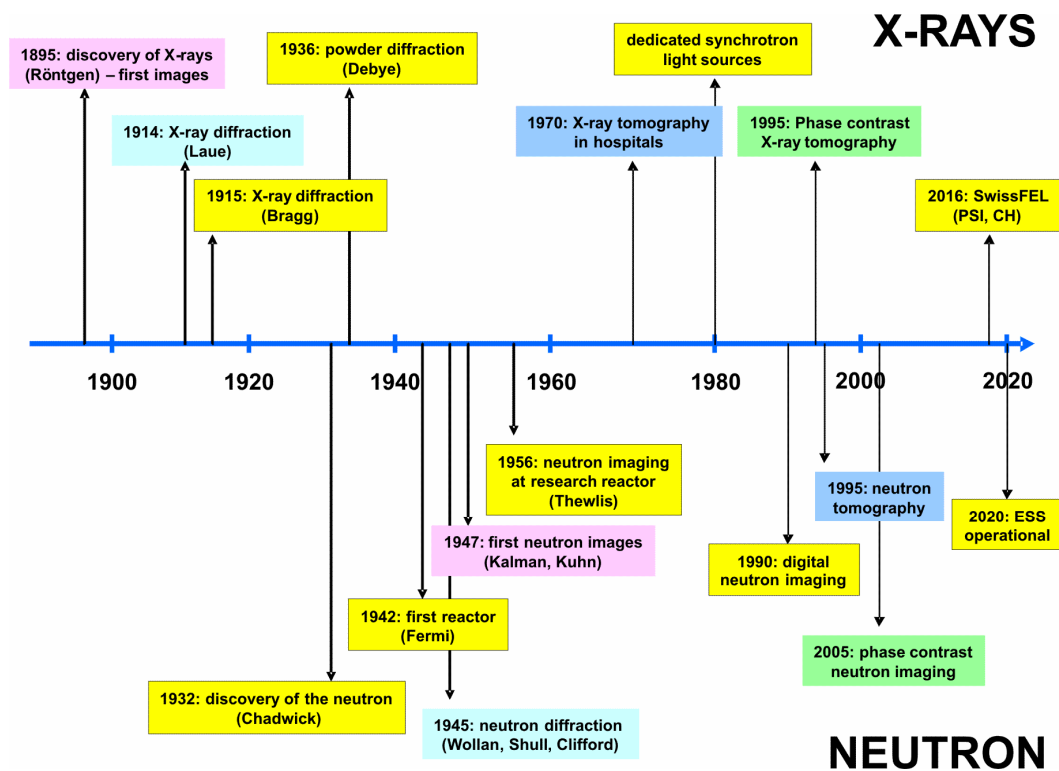

Fig.1:   *Historical overview in respect to X-ray and neutron imaging aspects (selection of facts)*

Diffraction and other kinds of scattering methods with neutrons were introduced into material research according to the availability of suitable sources. Neutron scattering has become an established research field by using reactor sources like at ILL (Grenoble) or FRM-2 (Munich) and at other prominent places around the world. About 250 reactor and accelerator based neutron sources are counted by the IAEA [1] in 2010.

X-ray sources on the basis of tubes are limited in intensity and flexibility. The invention and installation of electron accelerators for the production of synchrotron light have been a huge step forward for the X-ray diffraction and imaging community in order to increase the performance and enabled many new techniques. This development will be topped at some places by means of free electron laser facilities, preferentially working in the time domain.

On the other hand, it was another revolutionary step forward to enable the detection of the radiation with digital systems of much higher performance than films. In particular, the imaging techniques for both neutrons and X-rays took profit from this development and can provide today a large variety of new methods with high potential in many applications.

Fig. 1 summaries some most important inventions and activities in respect to X-ray and neutron research since the discovery of these radiations.

This article intends to describe some basics in respect to modern imaging techniques using X-rays, neutrons and synchrotron radiation. Based on the principle of interaction of matter with the different kinds of radiation it will be explained which information can be obtained by the inspection of material samples.
Technical details about facilities, imaging techniques and current applications will be given on the basis of the author's experiences at the installations at Paul Scherrer Institut (Switzerland).
The outlook is focussed on new trends in the methodical developments, the installation of new imaging systems and the creation of new application fields.

2   Basic principles

All transmission radiation techniques (with neutrons, X-rays and synchrotron radiation) are based on the same principle. A specially tuned beam of the radiation is selected from the source by means of collimator devices and filters. After the interaction with the object of interest the transmitted radiation is detected with a two-dimensional area detector, sensitive for the specific kind of radiation. This procedure is schematically described in Fig. 2.

Two beam geometries are interesting for practical applications: a parallel beam which allows a 1:1 shadow image of the object without geometrical blurring and a cone beam with a narrow focussing source point which enables a magnified image of the object. In reality, both approaches can only be made available with compromises due to the limitation of the radiation sources (source size and intensity). A collimation ratio CR can be defined as:

$$CR = \frac{L}{D} \qquad (1)$$

D corresponds to the size of the primary aperture and L to the length of collimation between the aperture and the detector. This number should be larger than 100 in order to obtain reasonable spatial resolution. The geometric blurring u is related to the sample-detector-distance d like:

$$u = \frac{d}{CR} \qquad (2)$$

The obtained field-of-view (FOV) is given by the beam size and should be at least as large as the detector area. It depends on the object size and its composition which detector area is most suitable for the investigation with the particular kind of radiation – see below.
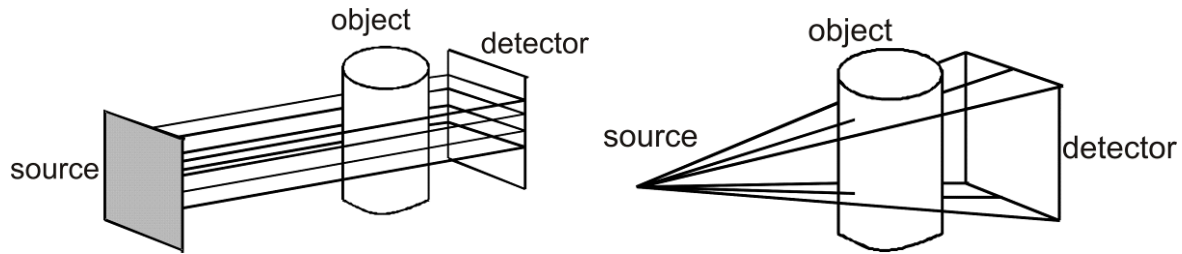

Fig. 2: *The principles in transmission radiation imaging: parallel beam (left); cone beam (right)*

For a quantitative approach in the transmission imaging techniques, the exponential attenuation law according to Beer - Lambert has to be taken into account:

$$I(x,y,E) = I_0(x,y,E) \cdot e^{-\Sigma(x,y,E) \cdot d(x,y)} \qquad (3)$$

The intensity of the initial beam I_0 arriving at a position in x and y into the z direction with an energy distribution around E is related to the transmitted beam I according to that exponential law. The exponent is given by the material thickness d in beam direction z and the attenuation coefficient Σ which is a material parameter with a high dependence on the beam energy.

The interaction of X-rays (and synchrotron radiation) with matter takes place in the electron shell of the atoms (mainly Compton scattering and photo-electron emission). Therefore it is understandable that atoms with fewer electrons in their shell interact only weakly with X-rays than these of heavy elements. The principle energy dependency of the attenuation for X-rays in the range between 1 keV and 100 MeV is shown with the example of Al in Fig. 3. The logarithmic scale has to be taken into account. Other materials have a similar slope but show different absolute values.

It is common to list the X-ray data for the attenuation coefficients with μ (unit cm^{-1}) or sometimes with μ /ρ (ρ=material density) as mass-attenuation coefficient (unit cm^2/g). In the case of neutron interactions Σ is called macroscopic cross-section (unit cm^{-1}) which is related to the tabulated microscopic cross-sections σ as follows:

$$\Sigma = N \cdot \sigma = \frac{\rho \cdot L}{M} \cdot \sigma \tag{4}$$

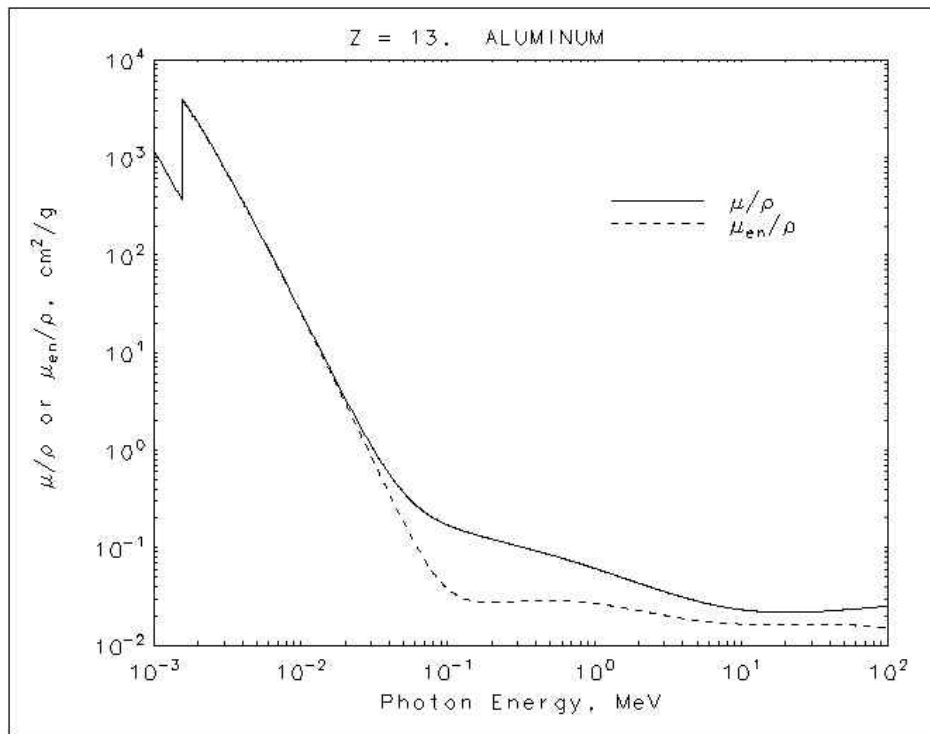N corresponds to the density of nuclei, M is the atomic weight and L the Avogadro's constant.

Fig. 3: *Mass-attenuation coefficients for Al of X-rays in the energy range between 1 keV and 100 MeV; source NIST [2]*

Neutrons (and in particular thermal and cold ones) interact only with the atomic nuclei and ignore the electrons in the shell completely. They can either be captured or scattered (in some few cases they induce fission). The interaction probability with matter is depending not only on the elements but also on the special isotope because the interaction with the nuclei can be very specific. For natural elemental compositions the attenuation probability the situation is shown in Fig. 4 – in comparison to the similar X-ray data.

It has to be highlighted that neutron interaction probabilities (described by the attenuation coefficients) does not underlie a systematic law when different materials are compared. There are prominent neutron absorbing isotopes (He-3, Li-6, B-10, Gd-157, …) whereas some other materials only weakly interact with neutrons (Pb, B-11, He-4, Zr). The strong absorbers are used as materials for neutron detection (see below).

In this respect, it depends on the material composition and the sample dimensions which radiation (X-rays or neutrons) have to be taken for the investigation best. The numbers in Fig. 4 can be taken directly to check the transparency of the material layer under investigation. According to (3), they describe to which intensity the beam drops down after passing a sample with the thickness of 1 cm.

Figure (top): X-ray values per element (1 cm thickness)

Period / Group	1	2	3	4	5	6	7	8	9	10	11	12	13	14	15	16	17	18
1	H 0.02																	He 0.02
2	Li 0.06	Be 0.22											B 0.28	C 0.27	N 0.11	O 0.16	F 0.14	Ne 0.17
3	Na 0.13	Mg 0.24											Al 0.38	Si 0.33	P 0.25	S 0.30	Cl 0.23	Ar 0.20
4	K 0.14	Ca 0.26	Sc 0.48	Ti 0.73	V 1.04	Cr 1.29	Mn 1.32	Fe 1.57	Co 1.78	Ni 1.96	Cu 1.97	Zn 1.64	Ga 1.42	Ge 1.33	As 1.50	Se 1.23	Br 0.90	Kr 0.73
5	Rb 0.47	Sr 0.86	Y 1.61	Zr 2.47	Nb 3.43	Mo 4.29	Tc 5.06	Ru 5.71	Rh 6.08	Pd 6.13	Ag 5.67	Cd 4.84	In 4.31	Sn 3.98	Sb 4.28	Te 4.06	I 3.45	Xe 2.53
6	Cs 1.47	Ba 2.73		Hf 19.70	Ta 25.47	W 30.49	Re 34.47	Os 37.92	Ir 39.01	Pt 38.61	Au 35.94	Hg 25.88	Tl 23.23	Pb 22.81	Bi 20.28	Po 20.22	At -	Rn 9.77
7	Fr -	Ra 11.80		Rf -	Db -	Sg -	Bh -	Hs -	Mt -	Ds -	Rg -	Uub -	Uut -	Uuq -	Uup -	Uuh -	Uus -	Uuo -

Lanthanides	La 5.04	Ce 5.79	Pr 6.23	Nd 6.46	Pm 7.33	Sm 7.68	Eu 5.66	Gd 8.69	Tb 9.46	Dy 10.17	Ho 10.17	Er 11.70	Tm 12.49	Yb 9.32	Lu 14.07
Actinides	Ac 24.47	Th 28.95	Pa 39.65	U 49.08	Np -	Pu -	Am -	Cm -	Bk -	Cf -	Es -	Fm -	Md -	No -	Lr -

Figure (bottom): Neutron values per element (1 cm thickness)

Period / Group	1	2	3	4	5	6	7	8	9	10	11	12	13	14	15	16	17	18
1	H 3.44																	He 0.02
2	Li 3.30	Be 0.79											B 101.6	C 0.56	N 0.43	O 0.17	F 0.20	Ne 0.10
3	Na 0.09	Mg 0.15											Al 0.1	Si 0.11	P 0.12	S 0.06	Cl 1.33	Ar 0.03
4	K 0.06	Ca 0.08	Sc 2.00	Ti 0.60	V 0.72	Cr 0.54	Mn 1.21	Fe 1.19	Co 3.92	Ni 2.05	Cu 1.07	Zn 0.35	Ga 0.49	Ge 0.47	As 0.67	Se 0.73	Br 0.24	Kr 0.61
5	Rb 0.08	Sr 0.14	Y 0.27	Zr 0.29	Nb 0.40	Mo 0.52	Tc 1.76	Ru 0.58	Rh 10.88	Pd 0.78	Ag 4.04	Cd 115.1	In 7.58	Sn 0.21	Sb 0.30	Te 0.25	I 0.23	Xe 0.43
6	Cs 0.29	Ba 0.07		Hf 4.99	Ta 1.49	W 1.47	Re 6.85	Os 2.24	Ir 30.46	Pt 1.46	Au 6.23	Hg 16.21	Tl 0.47	Pb 0.38	Bi 0.27	Po -	At -	Rn -
7	Fr -	Ra 0.34		Rf -	Db -	Sg -	Bh -	Hs -	Mt -	Ds -	Rg -	Uub -	Uut -	Uuq -	Uup -	Uuh -	Uus -	Uuo -

Lanthanides	La 0.52	Ce 0.14	Pr 0.41	Nd 1.87	Pm 5.72	Sm 171.47	Eu 94.58	Gd 1479.0	Tb 0.93	Dy 32.42	Ho 2.25	Er 5.48	Tm 3.53	Yb 1.40	Lu 2.75
Actinides	Ac -	Th 0.59	Pa 8.46	U 0.82	Np 9.80	Pu 50.20	Am 2.86	Cm -	Bk -	Cf -	Es -	Fm -	Md -	No -	Lr -

Fig. 4: *Attenuation coefficients for X-ray (100 keV) – above - and thermal neutrons – below – in the unit cm^{-1} . While a systematic increase of the attenuation contrast occurs for X-rays, no simple and determined relation to the mass number can be seen for neutrons. It is the strength of neutrons to provide a high contrast for hydrogen and other light elements and a high transmission ability for heavy elements.*
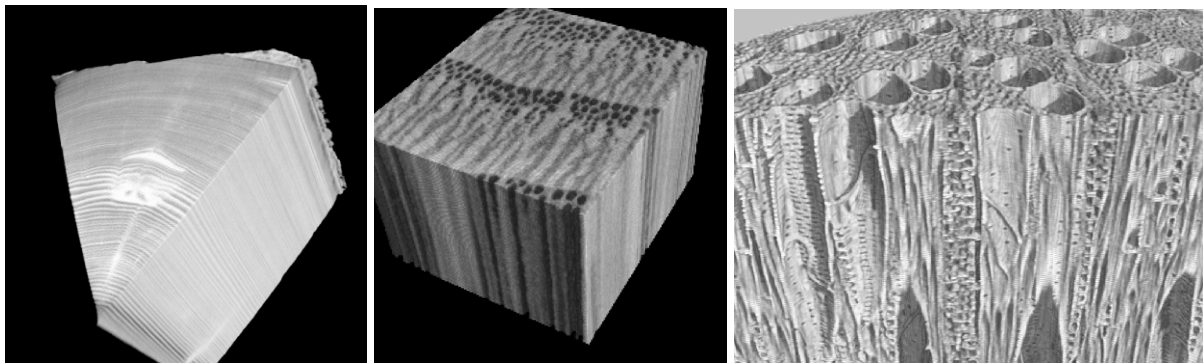
3   Application   Range   of   transmission   imaging techniques (example wood)

Fig. 5: *Tomographic views on wood samples on different size scale, obtained with X-rays (100 keV) – left; cold neutrons – middle; synchrotron light – right. The dimensions of the samples are – from left to right: about 10 cm, 1 cm, 1 mm.*

Although all three transmission techniques are performed at completely different facilities using at least two different kinds of radiation the findings about material properties can be quite specific in all three cases. This should be illustrated by a common material: wood.

As demonstrated in Fig. 5 with wooden samples of different sizes, structural information can be obtained with tomography methods (see below) in all shown 3 cases; however the details in respect to sample size and spatial resolution vary over 3 orders of magnitude. This behaviour is mainly caused by the attenuation of the applied beams given by the sample properties in respect to that radiation. In addition, the beam size and the inherent detector resolution contribute to the image features. While the attenuation coefficient for wood of X-rays of 100 keV is only 0.1 cm^{-1} it reaches 1.3 cm^{-1} for thermal neutrons. Accordingly, smaller samples with higher resolution and adequate contrast can be observed with neutrons. It has to be mentioned, that the interaction of neutrons with wood is mainly given by hydrogen, whereas in the case of X-ray mainly carbon and oxygen contribute to the image contrast and hydrogen plays nearly no role.

Therefore, neutrons are preferentially be used to determine the water content in wood with high sensitivity and accuracy [3].

In the case of synchrotron light, structural information can be obtained with a resolution similar to that for electron microscopy – however in 3D and without specific sample

preparation. Here the contrast is obtained by choosing photon energies of only few keV where the attenuation coefficients reach higher values too (see e.g. Fig. 3)
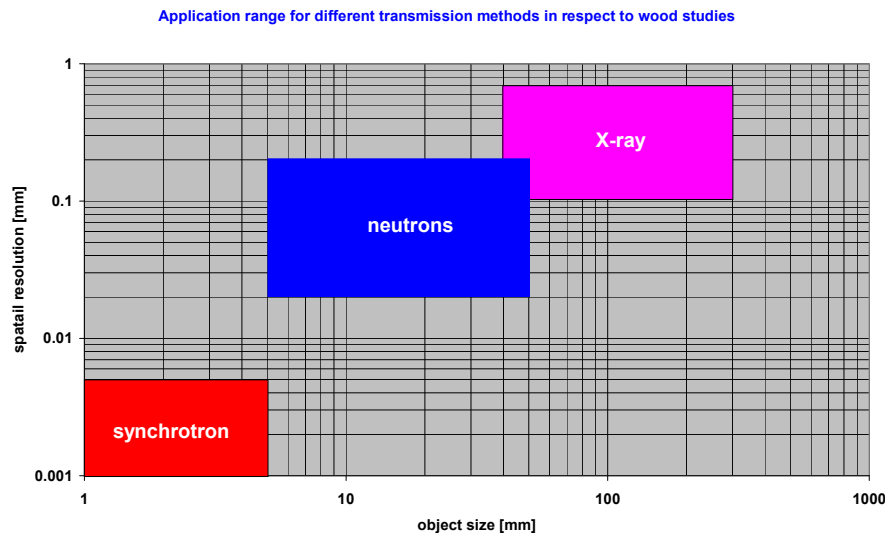
Application range for different transmission methods in respect to wood studies

Fig. 6: *The use of X-rays, neutrons and synchrotron radiation can cover a wide range of object size. This behaviour is given by the attenuation properties of wood in respect to the applied radiation, the beam conditions and the detector properties.*

4   Imaging Facilities

As shown simplified in Fig. 2, the setup for imaging consists of the source and the detector (behind the object). In reality, the equipment has to be surrounded by a suitable shielding as all three kinds of radiation have certain impact to human health depending on the dose. While X-ray imaging facilities can be found with different size and source strength in laboratories, neutrons and synchrotron radiation for imaging purposes have to be produced by large scale facilities. PSI (Switzerland) is operating two such units: SINQ – a steady state spallation neutron source and SLS – a third generation synchrotron light source. Both are equipped with imaging beam lines as it will be shown below.

4.1   X-rays

The generation of X-rays has been done since Röntgen's discovery according to the same principle: electrons are accelerated within an electric field of high voltage (some kV) and stopped on a metallic plate, the anode. Photons are emitted about perpendicular to the electron beam direction with energies below that high voltage level such counted in the unit keV (see the principle in Fig. 7 on the left). Beside this so called "Bremsstrahlung", photons with a characteristic energy are emitted too which corresponds to the levels in the different atomic shells of the anode material when an electron is removed from that shell and replaced by another one, accompanied by the photon emission. A typical photon emission spectrum is shown in Fig. 8.
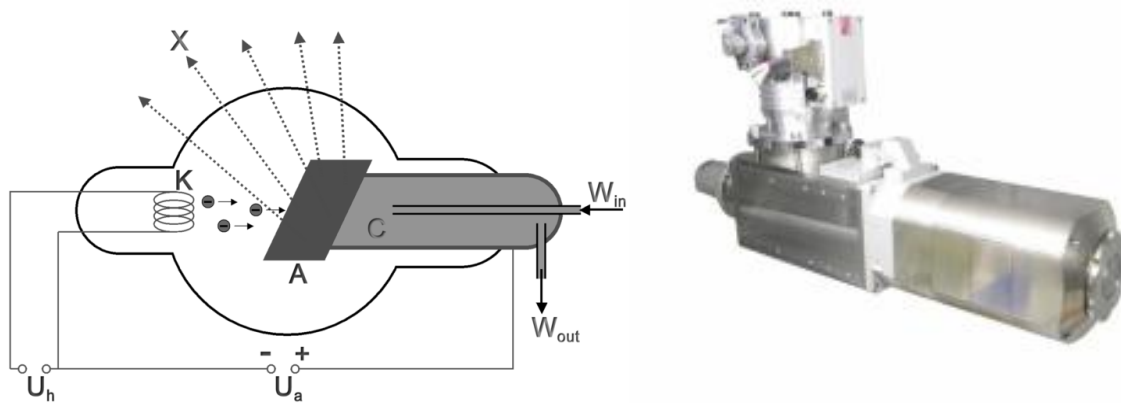
Fig. 7: *The principle of an X-ray tube (left): electrons are accelerated in an electrical field and photons with energies in the keV range are emitted from the anode. A state-of-the-art micro-focus tube is show on the right.*
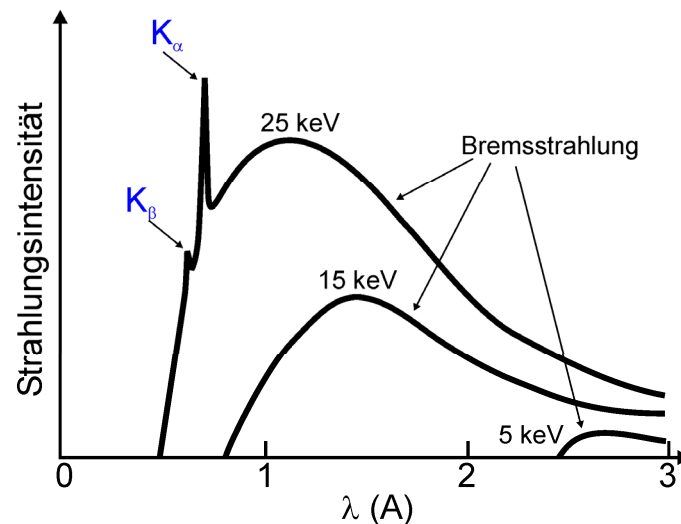

Fig. 8: *The emission spectrum of an X-ray tube consists mainly of the "Bremstrahlung" – a continuous spectrum until limits given by the high voltage. The characteristic lines exited in the anode material are overlaying the continuous part.*

X-ray imaging has been very common in medical diagnostics in the radiography mode since Röntgen's days until today. X-ray films have been used routinely where soft tissue occurs transparent and heavier parts of the body (e.g. bones) deliver higher contrast.

The step to digital X-ray imaging by using new types of image detectors enables nowadays also methods like tomography, laminography or real-time imaging.

X-ray imaging is used today more and more as research tool and as method for non-destructive testing in industry. Here, different and higher demands for advanced imaging systems came up. In particular for metallic objects, higher photon energies are required and tube voltages up to 420 kV become quite common.

On the other hand, images with much higher spatial resolution are possible if options for image magnification are taken into account. Using a cone beam setup (see Fig. 2, right), the small point source enables manifold magnification when the object is set close to the source, but the detector further away from the object. Finally, the resolution is given by the focal spot of the source which can be in the order of few micro-meters only. These tube systems are highly sophisticated as the source power and the heat removal have to be balanced in the right way.

Even if the advanced micro-systems have reached a very high level in spatial resolution they can not fully compete to the imaging systems at synchrotron light sources. In particular, their source strength is orders of magnitude smaller compared to the synchrotron sources ending up in much longer acquisition times.

4.2 Neutrons

Neutron imaging is much less available than that with X-rays since a beam line at strong neutron source is required. Either fission reactors or spallation neutron sources have been used for this purpose while radioactive sources are much too weak for practical use. A few accelerator devices started with neutron imaging capabilities. Due to the small number of such strong sources and the limited access to beam ports, there are only 10 to 15 competitive neutron imaging beam lines available world-wide (see Appendix).

In respect to image contrast, transmission and image quality, thermal or cold neutrons have been found most useful. Fast neutrons are less common since they provide inherent blurring in the detector even if they can transmit often thicker layers of materials.

A typical neutron imaging beam line layout is given schematically in Fig. 9. The fast neutrons from the initial source have to be slowed down in a moderation process by either hydrogen or deuterium before a part of the thermalized neutrons is extracted and guided to the sample. The transmitted neutrons are either measured in the detector behind the object or stopped in the beam dump.
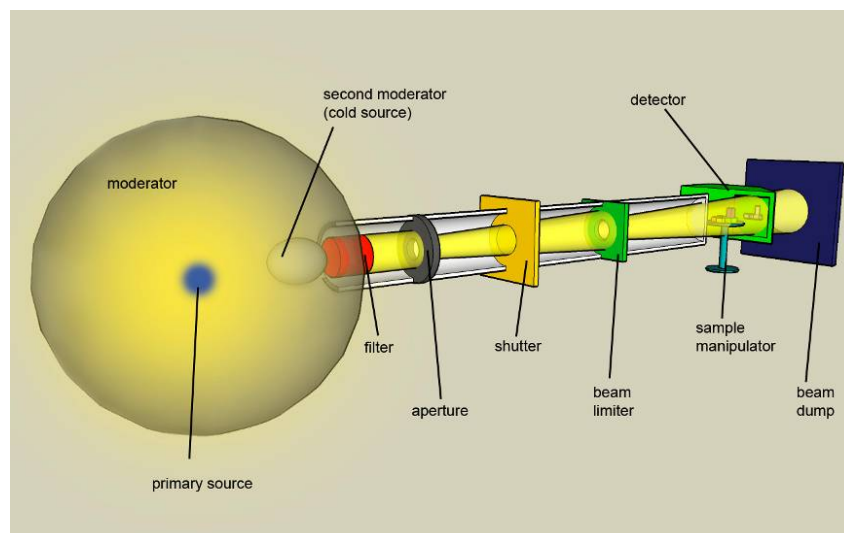

Fig. 9: *Layout of a beam line for neutron imaging describing the different components: the length is typically in the order of 10 meters, the beam size about 20 cm and can be varied.*
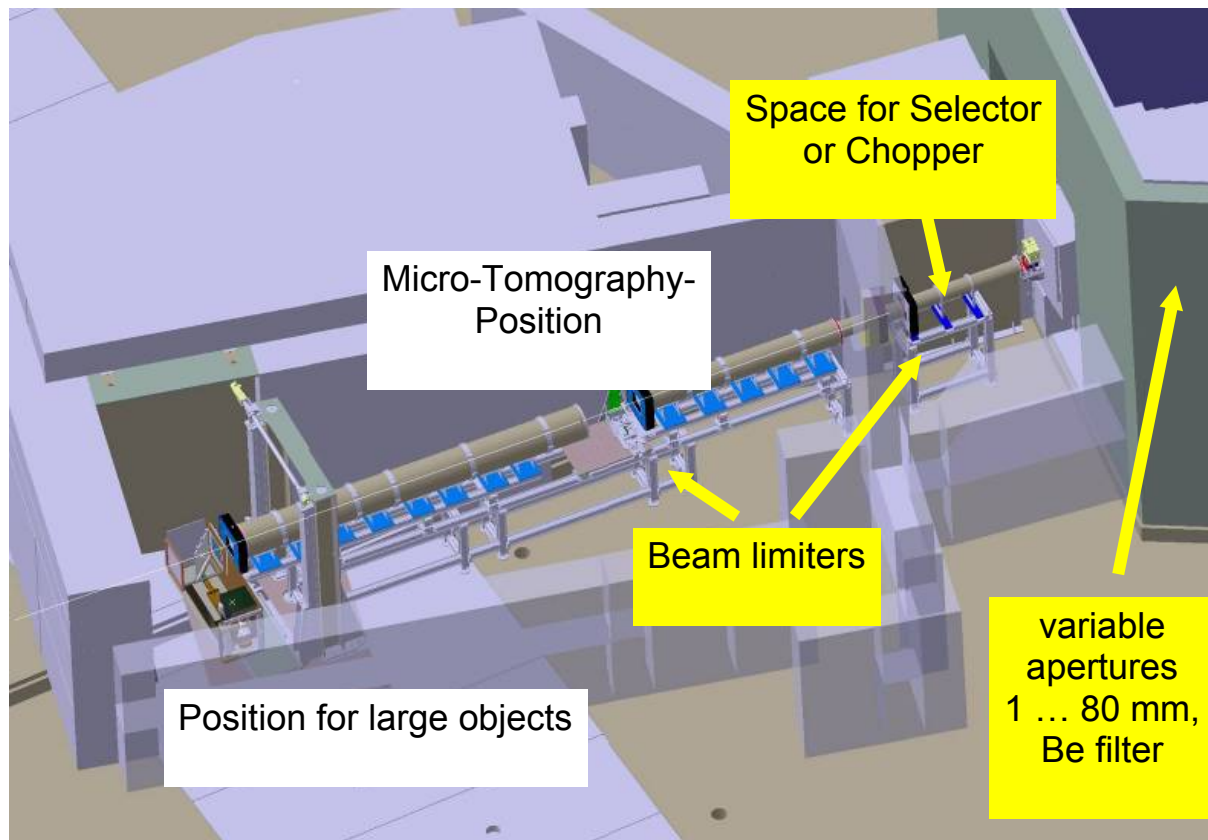
Fig. 10: *The ICON facility at SINQ (PSI, Switzerland) for imaging with cold neutrons; the length of the beam tube is about 12 meters; the aperture can be changed remotely controlled in steps from 1 mm to 80 mm.*

Based on this principle a facility as shown in Fig. 10 with the example of ICON at PSI can be realized. It should be built quite flexible in order to satisfy the demands of the different facilities users in respect to beam size, intensity and divergence. Accordingly, different detection systems have to be installed and used for the specific applications (see below).

4.3   Synchrotron radiation

Synchrotron light is emitted when charged particles (preferential electrons) with high energy are caused to change their direction by means of magnetic fields. Photons with keV energies are sent out into the initial direction of the charged particles. This previously misleading effect has been used to build dedicated large ring accelerators for electrons hosting many beam lines for X-rays aligned in tangential direction to the annular electron accelerator.

The intensity of such extracted beams of X-rays is by orders of magnitude higher in comparison to X-ray tubes. It can be tuned in several respects: collimation, coherence, spot size, energy band and intensity.

Facilities for imaging purposes are placed at several synchrotron light sources (see Appendix). As an example, the layout of the TOMCAT beam line [4] at SLS, PSI, CH is

shown in Fig. 10. The high intensity of the beam can be used either to create images with superior spatial resolution (far below 1 μm) or obtain image sequences (also in tomography mode) with extremely high frame rate. The beam size is in the order of few mm only which limits to applications of microscopically small samples (e.g. Fig. 5 – right).
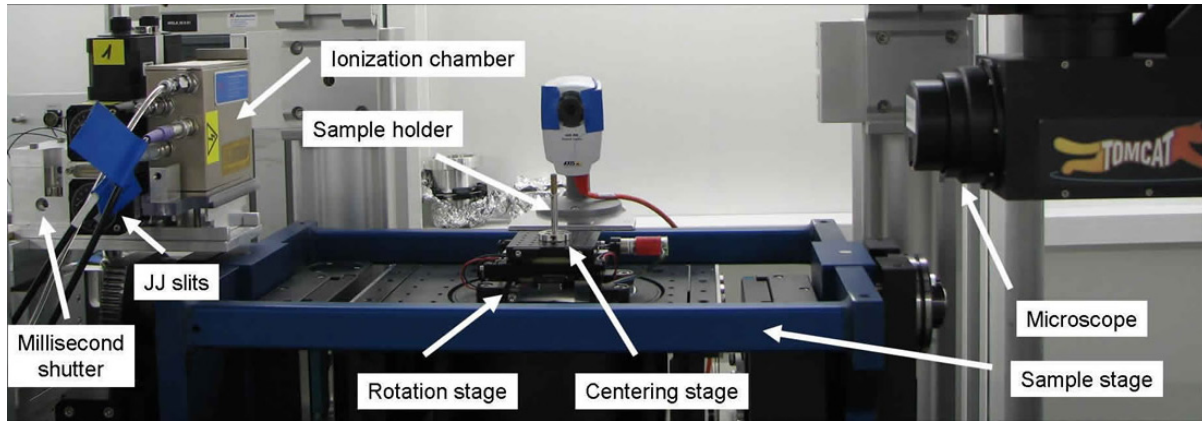

Fig. 11: *The TOMCAT imaging facility at the SLS synchrotron light source [4] (PSI, Switzerland) with some of the components described*

4.4 Imaging detectors

Film methods were used exclusively in the very beginning of transmission radiography. Although its inherent resolution is quite high there are many limitations in respect to the dynamic range, the linearity, the sensitivity and the missing options for data treatment. In the 90ies of last century, several digital imaging systems were invented and implemented. As primary radiation detection system scintillator screens, semi-conductor arrays or imaging plates have been used [5].
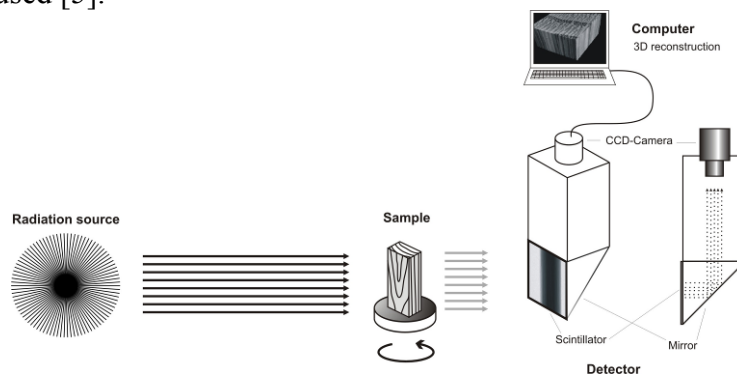

Fig. 12: *The setup of a digital imaging system based on a CCD camera observing the light from a radiation sensitive scintillation screen; under modified and specially arranged conditions this setup is in use for neutrons and X-rays as well*

Relatively simple, but flexible and most efficient is the combination of a highly sensitive camera (mainly CCDs, now also CMOS) with a radiation sensitive scintillation screen. A

typical setup is shown in Fig. 10, where the light from the scintillator is reflected out of the direct beam towards the camera, which is protected from direct irradiation in this manner.

Depending on the beam intensity, the exposure time with camera based systems is in the order of only seconds compared to minutes when a film has to be exposed. The result of imaging with digital systems is a data set containing a pixel matrix of grey values. State-of-the-art systems work with 16 Bit dynamic range enabling to distinguish more than 65.000 grey levels.

X-rays are able to excite detection systems mentioned above directly. This is not the case for neutrons due to their missing electric charge. A primary ionisation in the detector material is not possible therefore. Neutron detection has to be done via a nuclear reaction, mainly neutron capture. For this purpose, the following materials are in use mainly: Li-6, B-10, Gd and He-3. The reaction products – ions, α-particles, conversion electrons or gamma radiation – induce in a second step the measurable signal. For neutron imaging most common are scintillators in a combination of Li-6F mixed with ZnS [6].

Semiconductor arrays as pixel detectors [7] or amorphous silicon flat panels and imaging plates are in use as imaging devise beside camera detection systems. More advanced systems [8] are able to cover a high spatial resolution and high temporal resolution which can be used for an energy selection in the time-of-flight mode (see below).

5   Imaging techniques

The imaging with all three kinds of radiation has similarities and specific differences. In the "normal" radiography mode, the obtained image is an overlay of all material information in beam direction. For flat slabs there is no problem to distinguish the material distribution which is set "transparent" by the transmitting radiation. An example is given for the case of a hard disk drive with a more flat structure. Characteristic differences between X-ray and neutron imaging can be found whereas the inherent image quality is about the same.
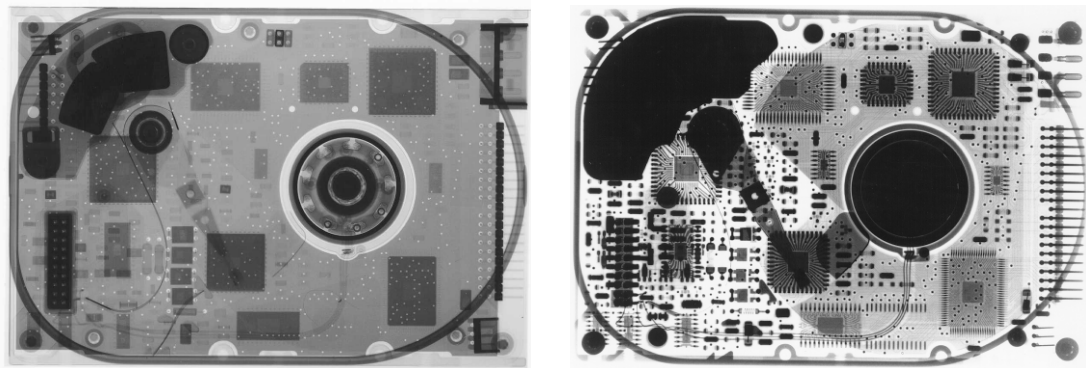

Fig. 13: *Neutron transmission radiography image (left) compared to an X-ray image (right)*
            of a hard disk drive: metallic parts are more transparent for neutrons whereas a
            higher contrast is obtained for the organic material of the conductor board.

5.1   Tomography

The third dimension of an object under investigation can be explored with the help of tomographic methods. For this purpose, information has to be derived from different orientation of the object, that means projection have to be taken from different viewing angles while the object is rotated around a well aligned vertical (or horizontal) axis.

Meanwhile the reconstruction methods, mainly based on filtered back-projection and implemented in several software tools are able to convert the projection data via sinograms into the volume data of the object as a matrix of voxel values in the format of attenuation coefficients (see (4)). All reconstruction algorithms are based on the assumption of the validity of that law over all dimensions of the object what is true only in first order.

If the volume data are available, software tools for visualisation and evaluation can be used for arbitrary virtual slices through the object and the separation of zones with the same attenuation contrast in segmentation routine. An example is given in Fig. 14 for a Buddha sculpture from the 14th century imaged in neutron radiography and tomography mode. In this case, the inner organic content (wooden stick, a wire, textiles, plants and seeds) can be visualized within the metallic cover – a case where neutrons exclusively have to be applied [9].

Fig. 14: *Comparison between a transmission neutron radiography image (middle) of a Buddha sculpture (Buddha Sakyamuni) from the 14th century (left) with a virtual slice derived from the tomography data set (right).*

Nowadays, tomography techniques are common with all three considered techniques. Based on the considerations in chapter 2 and 3 it has to be decided which method has to be used in respect to the required spatial resolution and its contrast. Compared to a simple transmission image, tomography requires about 300 – 500 times more acquisition time and a lot more effort for volume reconstruction and data visualization. The data to be stored and managed are in the GBytes region and a suitable data handling system is required.

5.2   Time-dependent studies

The study of processes in the time domain is very important with transmission radiation which can visualize inner structures and their sequential development. Generally, it depends on the beam intensity which degree of time resolution can be obtained. In this respect, synchrotron radiation is a favourite to provide the best conditions.

In respect to neutron imaging, the limitation to flux levels in the beam of 10^8 to 10^9 cm^{-2}s^{-1} in best cases is a real handicap. Considering a pixel size of 0.5 mm * 0.5 mm as reasonable and assuming a 100% detector efficiency for the flux of 10^9 cm^{-2}s^{-1} the time per frame cannot be better than 0.4 milliseconds when about 1000 counts are needed for a valid contrast. This performance can be obtained on only few places word-wide. In most cases, acquisition times of several seconds per frame are common. Beside the acquisition time, the read-out from the detector is quite critical and can take several seconds too.

For real applications there are two types of approaches:

1. Fast sequences of frames with limited image quality which is given by the compromise between the acquisition time and the detector noise. The typical frame rate (for neutrons) is in the order of 3 to 50 fps, depending on the beam intensity.
2. Stroboscopic imaging of repetitive processes where a stack of partial images is build to reach the best image quality from a very narrow time frame (e.g. 10 μs) – integrated over several thousands of cycles. An example is given in Fig. 15 for a running combustion engine under full load on 8000 rpm.
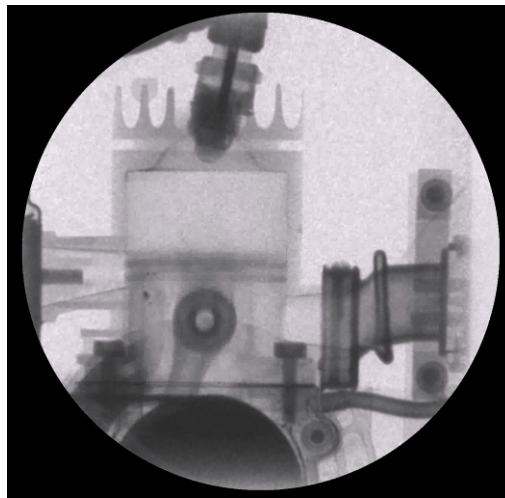

Fig. 15: *Investigation of the operation within a combustion engine in the real-time mode where the repetitive process is imaged through the metallic structure by means of neutrons. The engine was fired and operated on 8000 rpm, whereas a single frame was taken within 50 μs. Stacking about 1000 such identical images delivered the valid and useful information.*

Future application will be found at pulsed neutron sources where the neutron spectrum is spread over a certain range in the time domain, which brings us to energy-selective studies (see below).

5.3   Energy selection

The radiation sources emit primarily a brad spectrum of neutrons and X-rays, respectively. It is an advantage to apply only a narrow energy band of that radiation because the specific material properties can be enhanced. The attenuation cross-sections have quite strong energy dependence as shown in Fig. 2 for X-rays and for some structural materials in the energy range of "cold neutrons" (Fig. 14). The application of a broad spectrum of radiation averages and smooths the specific desired material behaviour in some respect and cases.
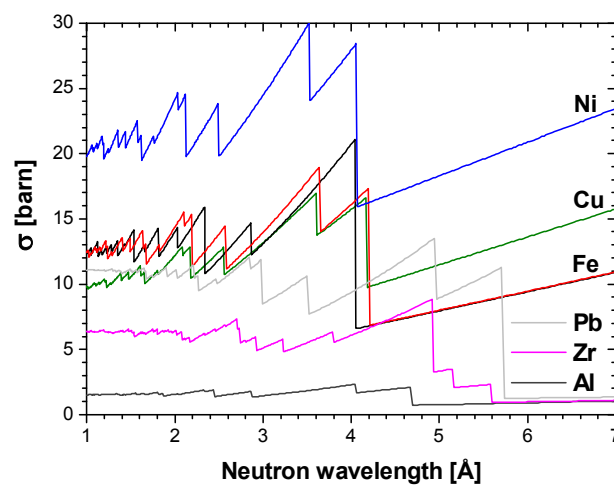
Fig. 16: *Microscopic cross-sections of crystalline structural materials in the cold neutron energy range are showing the characteristic Bragg edges caused by the neutron scattering at crystal lattice planes.*

Energy selective investigation can enhance the contrast between different materials when the right energy is chosen close to one or the other Bragg edges. Image referencing between two images at the same spatial position but taken with two different energies can further enhance the contrast by image post-processing techniques.

Because the Bragg behaviour is caused by the crystalline structure of the investigated materials the orientation and crystal distribution can be visualized directly in cases when the crystal size fits to the spatial resolution of the imaging system. Such an example is given in Fig. 17, where the laminar structure of a rolled Al sample becomes visible. At least three zones with different crystal structure (not composition!) can be distinguished. In poly-chromatic mode and in the absorption range above 5 Å the sample looks quasi-homogenous. This method can be used for a pre-characterisation of unknown materials in a simple and non-destructive way.
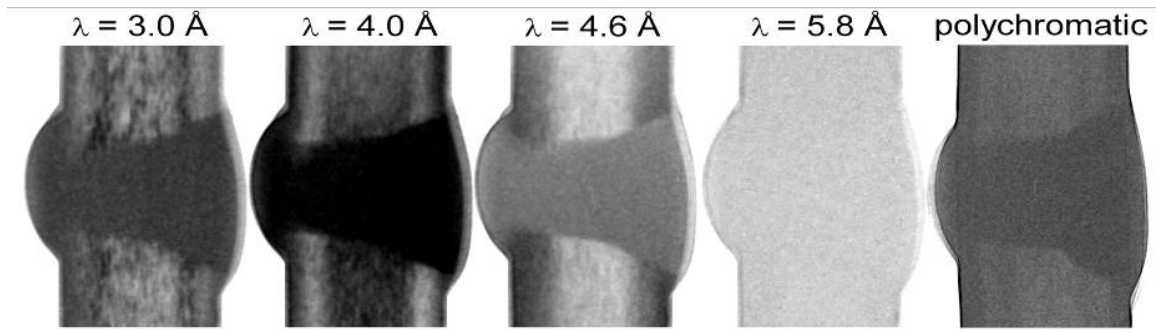
Fig. 17: *Part of a rolled Al plate with a weld in the middle was studied at different neutron energies and structural differences can be derived in the plate but not in the weld where the grain size is too small compared to the detection limits.*

Presently used devices for energy selection (turbines, mono-chromatizers) are able to cut out energy bands of 5% to 15%, depending on the specific performance parameters. With the help of the upcoming pulsed spallation neutron sources the time-of-flight options have much less limitations and will allow the selection of narrower band width.

5.4 Phase contrast imaging

Nearly all results of investigations described above were based on attenuation in the absorption contrast mode even if scattering of neutrons or photons might play a major role. In this way, all radiation which is lost in the direct beam behind the object is handled in the attenuation law equally.

However, neutrons have also wave properties like X-rays. In the case of the neutrons, their wavelength λ can be calculated according to de Broglie's formula:

$$\lambda = \frac{h}{m \cdot v} \tag{4}$$

with h as the Planck's constant, m the neutron mass and v its velocity. One important feature of the interaction of waves with matter is refraction. The wavelength is changed as in classical optics and an index of refraction n (ratio between the velocities inside and outside the object) can be derived to depend on the wavelength and the cross-section of the coherent scattering:

$$n = \frac{v_i}{v_0} = 1 - \delta = 1 - N \cdot \sigma_{coher} \cdot \lambda^2 / 2 \cdot \pi \tag{5}$$

In reality, δ is in the order of 10^{-5} only and can be either positive (e.g. for Al, Cu, Fe) or even negative (e.g. for Ti or Mn).

This little phase shift can be used in practical imaging to enhance the contrast at edges in order to distinguish materials with the same attenuation behaviour but different refraction properties. Detection systems with high spatial resolution are needed to take profit from this behaviour. An example from neutron edge enhancement by refraction is shown in Fig. 18.
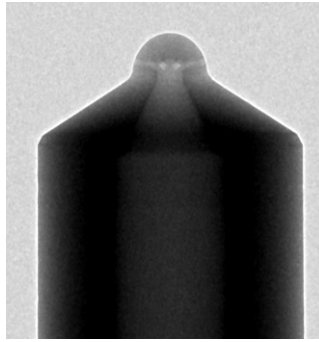
Fig. 18: *Upper part of a Diesel injection nozzle observed with cold neutrons and a high resolution imaging detector; the edge enhance effect is clearly visible caused by the refraction in steel; sample diameter 4 mm.*

Beside that edge enhancement, it was possible to derive the differential phase information by special experimental setups with a grating interferometry technique [10] as an additional material parameter. This technique is now available in X-ray systems and at cold neutron beams as well.

6   Applications

Practical applications in transmission radiation imaging for non-invasive investigations of objects are progressively in use in different fields of science and engineering. It is the increasing availability of X-ray systems in many labs and the strong improvement of digital imaging systems, including the computation and evaluation techniques which push this attractive field forward. Based on considerations about the attenuation behaviour of the sample material, the demands in resolution and the dimensional boundary conditions the best suitable setup has to be chosen.

6.1   Material research: metals, bio, geo-science

The complementarities between X-rays and neutrons were roughly explained in chapter 2. The consequence for practical applications can be seen e.g. in Fig.13: neutrons have in most cases higher penetration ability through metals while a strong contrast is given for hydrogenous materials even in a metallic cover. Therefore thin parts of an animal body can well be visualized in neutron tomography (see Fig. 19).

Unfortunately, the resolution in neutron imaging is presently limited to about 20 μm although the contrast might be high enough to see more details in biological samples. Studies with demand in higher resolution should be done with synchrotron radiation even the contrast might be quite low.

Studies with geological samples gained high interest because structural information on different size scale can be derived with tomography methods. An important feature is the study of the porosity and the interaction with water flow phenomena. Here, neutrons can provide high contrast even in small moisture contents. Finally, the behaviour of plant roots in soil were studied with success during the feeding with moisture and nutrients [11].

Fig. 19: *Tomographic views onto a fly which was studied using cold neutrons with presently highest possible resolution (pixel size 13.5 μm; sample size12 mm); the advantage of the high contrast for hydrogen enables to see very much detail – better than naked human eye can do.*

6.2   Industrial applications

Several industrial companies have started to install X-ray imaging systems for the inspection and quality insurance next to production lines or in dedicated in-house labs. Only if these installations fail to reach the inspection goals other techniques like neutron imaging or imaging with synchrotron radiation is taken into account. In these cases, the industrial partner needs to enter a large scale facility and has to book beam time on commercial basis.

In respect to neutron imaging there is a short list of prominent applications without any guarantee for completeness:

- Polymer Electrolyte Fuel Cells
- Combustion engine operation, fuel injection
- Batteries (Lithium-ion)
- Diesel particular filters
- Adhesive and brazing connections
- Welds in structural materials
- Explosives
- Two-phase flow processes
- Fuel and cladding for Nuclear Power Plants

There will be found several new applications for the different transmission imaging techniques, based on the permanently changing and increasing demands by industry. A high degree of flexibility is required in order to satisfy the demand in the right manner by further improvements in the experimental techniques.

6.3   Cultural heritage studies

The demands from museums and archaeologists to study and to visualize hidden structures and features in objects of cultural heritage value are mainly coupled with the need for a non-destructive or non-invasive approach because no damage is allowed. There is a tradition to

investigate museums objects with X-rays [12], but this cannot solve all request due to missing transmission, limited contrast and spatial resolution. Therefore, the availability of new imaging techniques with neutrons, synchrotron radiation and by using new imaging methods is very welcome by the art historical scene.

In the framework of this course only a few examples (e.g. Fig. 14) can be given. In some cases, the X-ray and neutron data fits well together to create a comprehensive picture of the object. In some other cases, only the one or other method can solve the task to visualize the important content. In the case in Fig. 14, X-ray would completely fail to see the inner content of the sculpture due to missing contrast for the organic content and limited transmission through the metallic cover of the statue.

7   Summary and Outlook

Transmission imaging techniques based on X-rays or neutrons are modern tools for research and technical applications. An enormous gain in performance happened in the last few years by the introduction of advanced digital systems, the implementation of sophisticated methods like phase imaging and tomography on routine operation base.

Already with table-top laboratory installations for X-ray tomography the resolution came close to the micro-meter region.

The highest possible performance can still be found at large scale facilities like synchrotron light sources and strong neutron sources. Their beams can be used to create highest resolution images, fast image sequences, energy dispersive images or images with superior dynamic and low noise.

However, there is still potential for further improvements by the implementation of better detection systems, methodical developments and the extension of the user application range. In this respect, the combination of imaging with diffraction and the direct combination of neutron with X-ray imaging are promising approaches. Another future trend will be the improvement in the energy resolution in neutron imaging my means of time-of-flight methods at pulsed sources.

Appendices

Facilities for transmission imaging with neutrons and synchrotron radiation world-wide

Country	Location	Institution	Facility	Neutron Source	thermal/cold flux [cm^{-2} s^{-1}]	L/D - ratio	Field of View
Austria	Vienna	Atominstitut	imaging beam line	TRIGA Mark-II, 250 kW	1.00E+05	125	90 mm diam.
Brazil	Sao Paulo	IPEN	imaging beam line	IEA-R1M 5 MW	1.00E+06	110	25 cm diam.
Germany	Garching	TU Munich	ANTARES	FRM-II 25 MW	9.40E+07	400	32 cm diam.
Germany	Garching	TU Munich	NECTAR	FRM-II 25 MW	3.00E+07	150	20 cm diam.
Germany	Berlin	HZB	CONRAD	BER-II 10 MW	6.00E+06	500	10 cm * 10 cm
Hungary	Budapest	KFKI	imaging beam line	WRS-M 10 MW	6.00E+05	100	25 cm diam.
Japan	Osaka	Kyoto University	imaging beam line	MTR 5 MW	1.20E+06	100	16 cm diam.
Japan	Tokai	JAEA	imaging beam line	JRRM-3M 20 MW MTR	2.60E+08	125	25 cm * 30 cm
Korea	Daejon	KAERI	imaging beam line	HANARO 30 MW	1.00E+07	190	25 cm * 30 cm
Switzerland	Villigen	PSI	NEUTRA	SINQ spallation source	5.00E+06	550	40 cm diam.
Switzerland	Villigen	PSI	ICON	SINQ spallation source	1.00E+07	350	15 cm diam.
USA	PennState Uni.	University	imaging beam line	TRIGA 2 MW	2.00E+06	100	23 cm diam.
USA	Gaithersburg	NIST	CNR	NBSR 20 MW	2.00E+07	500	25 cm diam.
USA	Sacramento	McCleallan RC	imaging beam line	TRIGA 2 MW	2.00E+07	100	23 cm diam.
South Africa	Pelindaba	NECSA	SANRAD	SAFARI-1 20 MW	1.60E+06	150	36 cm dia.

A: Prominent facilities for neutron imaging around the world

Country	Location	Institution	Facility	Source	Energy
Switzerland	Villigen	Paul Scherer Institut	TOMCAT	SLS	12-40 keV
USA	Upton	BNL	XCMT	ALS	6-36 keV
Germany	Karlsruhe	FZ Karlsruhe	TopoTomo	ANKA	> 6 keV
France	Grenoble	ESRF	ID22	ESRF	
Germany	Hamburg	DESY	P06	HASYLAB	
UK	Didcot	Rutherford Lab	I13L	DIAMOND	6-30 keV
Japan	Harima Science Park City	RIKEN	BL 20	SPRING 8	
USA	Chicago	ANL	5-BM-C and others	APS	
France	Saclay	France joint effort	PSICHE	SOLEIL	15-100 keV
Italy	Trieste	AREA Science Parc	SYRMEP	ELETTRA	

B: Prominent facilities for imaging with synchrotron radiation around the world (selection)

References

[1] RR data base IAEA: http://nucleus.iaea.org/RRDB/RR/ReactorSearch.aspx

[2] www.nist.gov/pml/data/xraycoef/index.cfm

[3] D. Mannes, Non-destructive testing of wood by means of neutron imaging in comparison with similar methods, Diss. ETH Zurich No. 18563, 2009

[4] www.psi.ch/sls/tomcat/beamline-layout

[5] E.H. Lehmann, A. Tremsin, C. Grünzweig, I. Johnson, P. Boillat and L. Josic, Neutron imaging — Detector options in progress, 2011 JINST 6 C01050

[6] G. Frei, E.H. Lehmann, D. Mannes, P. Boillat, The neutron micro-tomography setup at PSI and its use for research purposes and engineering applications, Nuclear Instruments and Methods in Physics Research Section A: Accelerators, Spectrometers, Detectors and Associated Equipment, Volume 605, Issues 1-2, ITMNR 08 - Proceedings of the sixth Topical Meeting on Neutron Radiography, 21 June 2009, Pages 111-114, ISSN 0168-9002

[7] E. H. Lehmann, P. Vontobel, G. Frei, C. Br.onnimann, Neutron imaging—detector options and practical results, Nuclear Instruments and Methods in Physics Research A 531 (2004) 228–237

[8] A.S. Tremsin, J.B. McPhate, E.H. Lehmann, J.V. Vallerga, O.H.W. Siegmund and W.B. Feller, High resolution neutron radiography with very compact and efficient neutron collimators, 2011 JINST 6 C01041

[9] E.H. Lehmann, S. Hartmann, M.O. Speidel, Investigation of the content of ancient Tibetan metallic Buddha statues by means of neutron imaging methods, Archaeometry 52, 3 (2010) 416-428

[10] Pfeiffer F., Gruenzweig C., Bunk O., Frei G., Lehmann E., and David C.
Neutron Phase Imaging and Tomography
PHYSICLAL REVIEW LETTERS 96, 215505, June 2, (2006)

[11] A. B. Moradi, A. Carminati, D. Vetterlein, P. Vontobel, E. Lehmann, U. Weller, J. Hopmans, H.-J. Vogel, S. Oswald, Three-dimensional visualization and quantification of water content in the rhizosphere, New Phytologist (2011) 192: 653-663

[12] J. Lang, A. Middleton, Radiography of Cultural Material, Elsevier, 2005, ISBN 0 7506 6347 2